

Trajectory Optimization Using Neural Network Gradients of Learned Dynamics

Nathanael Köhler, Bhavya Sukhija, Miguel Zamora, Simon Zimmermann, Stelian Coros

Abstract—Trajectory optimization methods have achieved an exceptional level of performance on real-world robots in recent years. These methods heavily rely on accurate physics simulators, yet some aspects of the physical world, such as friction, can only be captured to a limited extent by most simulators. The goal of this paper is to leverage trajectory optimization for performing highly dynamic and complex tasks with robotic systems in absence of an accurate physics simulator. This is achieved by applying machine learning techniques to learn a differentiable dynamics model of the system from data. On the example of a Radio-controlled (RC) car, we show that from data collected in only 15 minutes of human-operated interactions with the car, a neural network is able to model highly nonlinear behaviors such as loss of traction and drifting. Furthermore, we use the analytical gradients of the neural network to perform gradient-based trajectory optimization, both in an offline and online setting. We find that our learned model is able to represent complex physical behavior, like drifting and gives unprecedented performance in combination with trajectory optimization methods.

Index Terms—Motion and Path Planning, Machine Learning for Robot Control, Optimization and Optimal Control, Model Learning for Control.

I. INTRODUCTION

ROBOTS, in particular mobile robots, are expected to perform complex and highly dynamic maneuvers in unknown environments [1]–[5]. This can be achieved through traditional trajectory-based optimal control approaches, such as trajectory optimization [6]. Trajectory optimization methods are well established and give feasible trajectories which exhibit complex and dynamic behaviors [7]–[9]. The goal of this work is to leverage these techniques to accomplish highly dynamic tasks in complex settings with robotic systems. This imposes a challenge because the most successful trajectory optimization methods require an accurate enough differentiable model of the robot’s dynamics. For highly dynamic and complex settings, it is difficult, if not impossible, to obtain such parametric models. As an example, for race cars with high speeds and cornering accelerations, a model of the tire force and moment characteristics is required. Obtaining this model is very challenging, especially because such a model depends on multiple external factors like the temperature [10]. System identification [11]–[13] is a valuable technique, used to learn the model of the system from data. Using data collected on the system,

This work has been submitted to the IEEE for possible publication. Copyright may be transferred without notice, after which this version may no longer be accessible.

The authors are with the Department of Computer Science, ETH, Zürich, Switzerland. nate@striking.ch; sukhijab@ethz.ch; miguel.zamora@inf.ethz.ch; simon.zimmermann@inf.ethz.ch; scoros@gmail.com



Fig. 1: We aim to learn a physical model of a dynamic RC car and use the model in gradient-based trajectory optimization. Thanks to a high torque motor, the rear-wheel-driven RC car is able to perform drifting turns.

universal approximators such as multilayer feedforward neural networks [14] can be trained to capture its dynamics. Such a dynamics model can then be used for trajectory optimization. In practice, this imposes several challenges: (i) recording data on the system is time-consuming and can cause wear and tear to the system (ii) trajectory optimization schemes generally also require derivatives of the learned model with respect to the control vectors. These can be obtained for simple neural network architectures. But such architectures may fail to capture the true dynamics appropriately. On the other hand, for higher capacity architectures, overfitting the data might lead to noisy derivatives.

In this work, we investigate how high-capacity models like neural networks can be combined with traditional trajectory optimization schemes to perform highly *complex* and *dynamic* maneuvers with robots. We conduct these investigations on the example of a RC car for which we aim to perform *dynamic* drifting behaviors (see Fig. 1). The drifting maneuvers of a car are complex and difficult to model [15], [16]. Furthermore, the models typically require tuning that needs to be repeated for different grounds and tires. Therefore, we instead collect data directly on the car and use it for training a neural network

model to capture its dynamics. We propose an intuitive state space representation of the system which allows us to learn an accurate enough model after collecting only a small corpus of data consisting of *15 minutes* driven by a human operator. For the model selection, we leverage a simulation of the car to pick a model which (i) captures the dynamics of the car well enough and (ii) gives smooth derivatives that can be successfully used for trajectory optimization. Our results show that by considering *continuous* activation functions even a simple neural network model can be used for traditional gradient-based trajectory optimization methods. Furthermore, our results on hardware demonstrate that trajectory optimization with our learned model is able to perform complex tasks such as drifting on the real robot, which according to [16] usually requires expert drivers. This highlights the benefits of the synergy between traditional trajectory-based control methods and machine learning.

II. RELATED WORK

Nonlinear system identification is also used in model-based reinforcement learning (MBRL) [17]. Compared to model-free reinforcement learning methods, MBRL approaches are more sample efficient [18]. This is extremely important when working directly with real-world robots since it prevents hardware deterioration. MBRL has been successfully applied to a variety of robot control tasks in simulation and hardware [19]–[27]. In particular, [19]–[23] use gradient-based optimization schemes to obtain the control policy. Nonetheless, these methods either use parameterized models with hand-picked features [23] or Gaussian processes (GPs) [28] to learn the system dynamics. Hand-picking features is a time-consuming, often unintuitive, and sometimes also an impossible process. GPs on the other hand are powerful machine learning models that generalize well in the low-data regime. But they find it challenging to learn very complex and discontinuous dynamics [29], which are more and more common in robotics [30]. Therefore, as an alternative, neural networks have been considered [24]–[27]. They are capable of capturing complex behaviors and also scale well for high-dimensional settings. However, apart from a few notable exceptions [31]–[35], these methods mostly use population-based search heuristics such as the cross-entropy method [36], in contrast to gradient-based optimization schemes, to obtain a control policy. Population-based methods have two main advantages over gradient-based schemes: (i) they seek for the global optimum and (ii) they do not suffer from exploding and vanishing gradients over the rollouts [37]. Nevertheless, these methods are costly and do not scale well with the dimension of the horizon and action space, which hinders their application on real-world robots, where fast computations times are desired for feedback control (e.g., Model Predictive Control (MPC) [38]). Therefore, a gradient-based optimization scheme is often preferred for such applications. This requires additional considerations for the modeling. In particular, models that can not only capture the dynamics well but also provide useful derivatives with respect to the inputs are desired. An interesting approach is proposed in [39], where local linear time-varying models are learned

using linear regression with Gaussian Mixture Models and combined with linear-Gaussian controllers. Here, the optimal controller parameters are obtained using the iterative linear-Gaussian regulator (iLQG) [40] solver. However, the proposed models only represent the system locally. In our work, we demonstrate that even a “simple” neural network model with continuous activation functions is able to capture complex and highly nonlinear dynamics. Furthermore, our model also provides excellent performance in combination with gradient-based optimization on the RC car. This motivates further investigation on other dynamical systems for future work.

III. METHOD

Our overarching goal is to find an optimal control sequence for our dynamical system. We formulate this as a *time-discretized* trajectory optimization problem: Let $\mathbf{x} := (\mathbf{x}_1, \dots, \mathbf{x}_n)$ and $\mathbf{u} := (\mathbf{u}_0, \dots, \mathbf{u}_{n-1})$ be the stacked state and control vectors for a total of n trajectory steps. Given a known initial state \mathbf{x}_0 , we write the trajectory optimization problem as

$$\min_{\mathbf{x}, \mathbf{u}} \ell(\mathbf{x}, \mathbf{u}) \quad (1a)$$

$$\text{s.t. } \mathbf{x}_{i+1} = f(\mathbf{x}_i, \mathbf{u}_i), \quad \forall i = 0, \dots, n-1 \quad (1b)$$

with total cost ℓ and state transition function f . The latter models the dynamics of the physical system we want to control. As discussed before, we aim to model our dynamical system using a neural network, which we will discuss in the following.

A. Learned Car Model

We investigate our methodology based on a specific dynamical system, namely a radio-controlled (RC) toy car (see Fig. 1). The intuitive nature of this system enables us to run investigations in both simulation and the physical world. We note that although this system is comparably simple, it can exhibit highly dynamic behaviors (e.g. when performing drifting maneuvers), and we aim to capture these behaviors in our learned model.

We assume that the toy car exclusively drives on a planar ground. The state \mathbf{x}_i consists of three degrees of freedom, namely the car’s planar position as well as its orientation. The control input \mathbf{u}_i is two-dimensional, and consists of the acceleration applied on the back wheels (i.e. the “throttle”) and the steering angle of the front wheels. We note that as we aim to learn our model from data, it is impractical to express the state in terms of world coordinates, as it is not a pose-invariant parameterization. We learn the state in terms of local velocities expressed in the coordinate frame of the car. This reduces the state-space the neural network has to learn. We denote these local velocities at trajectory step i with \mathbf{v}_i , and consequently choose a state transition function (as given by Eq. (1b)) as

$$\hat{\mathbf{x}}_{i+1} = \mathbf{x}_i + hf_{\theta}(\mathbf{v}_i, \mathbf{u}_i) \quad (2)$$

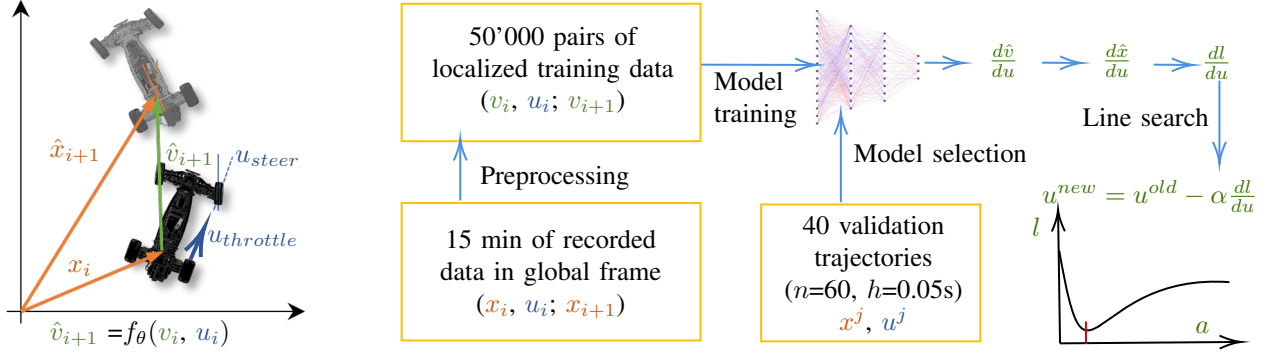


Fig. 2: Overview of the pipeline used for our experiments on the RC car. This includes (i) data collection, (ii) model training, (iii) and trajectory optimization.

with learned dynamics model f_θ , parametrized by θ , and time between two consecutive trajectory step h . The resulting optimization problem using the learned model is then:

$$\min_{\hat{\mathbf{x}}, \mathbf{u}} \ell(\hat{\mathbf{x}}, \mathbf{u}) \quad (3a)$$

$$\text{s.t. } \hat{\mathbf{x}}_{i+1} = \hat{\mathbf{x}}_i + h f_\theta(\hat{\mathbf{v}}_i, \mathbf{u}_i), \quad \forall i = 0, \dots, n-1 \quad (3b)$$

where $\hat{\mathbf{x}} := (\hat{\mathbf{x}}_1, \dots, \hat{\mathbf{x}}_n)$ is the concatenation of predicted states using the learned model.

As we want our system to perform dynamic maneuvers that involve loss of traction and drifting (see Fig. 1), we use an RC car with a high torque motor. As it is more convenient to record data and analyze the performance of a learned model in simulation, we employ a simple parameterized model that roughly matches the behavior of the real car. This allows us faster iterations when investigating different network architectures. Furthermore, it acts as a baseline when comparing the performance of different model choices in the context of trajectory optimization (section IV). We emphasize that we only use this model to analyze the efficacy of individual network design choices, and not to generate data to learn the behavior of the physical car. We provide a brief and intuitive description of the employed simulation model. Starting from simple driving dynamics (see e.g. [41]), we incorporate drifting behaviors as follows: First, we calculate the current local velocity for each wheel. Then, we compute the acceleration needed at each wheel to satisfy the no-slip condition. If the resulting acceleration per wheel exceeds a predefined static friction coefficient, it results in a loss of traction, which we incorporate by scaling down the accelerations to a lower dynamic friction coefficient. Finally, we apply the resulting changes to the car's state. We note that this simulation model was not designed to be physically accurate, but we find that it matches the physical counterpart well enough to make informed decisions for the network choices used to learn the behavior of the real car.

To train the model of the physical car, we collect data directly in the real world. Hereby we use a commercial, room-scale motion capture system to localize the car at a framerate of 240 Hz in an area of 5×10 meters. We recorded 15 minutes of training data plus 1 minute of test data. We recorded 40

additional validation trajectories of 3s each, that cover specific aspects of the RC cars dynamics such as standard driving with traction as well as intentional loss of traction (i.e. drifting). These trajectories are used to guide the selection of trained neural networks for the physical car, and we will further discuss this in section IV. We note that typical MBRL methods usually collect additional data after evaluating a control policy to further update and improve the model. In this work, we refrain from doing so, as we are interested in investigating how accurate a suitable dynamics model can be learned with minimal effort in terms of data collection and training.

We encounter significant noise in our recorded data, especially concerning the direction of the RC car. Therefore, during preprocessing, we employ a Savitzky-Golay smoothing filter [42] to reduce the noise. Then, we calculate local velocities based on the captured global pose using finite difference. Together with the recorded control input \mathbf{u}_i , this constitutes the data we train on. Hereby, we use feed-forward neural networks and experiment with different network sizes as well as activation and loss functions, which we will discuss in detail in section IV.

B. Control Costs

The total control cost $\ell(\hat{\mathbf{x}}, \mathbf{u})$ as introduced in Eq. (3a) is the sum of several individual costs. First of all, we define target states in global coordinates for predefined trajectory steps i , denoted by $\bar{\mathbf{x}}_i$. We match them with the corresponding trajectory states by employing a simple quadratic penalty

$$\ell_{\text{target}}(\hat{\mathbf{x}}) = \sum_{i \in I} \|\hat{\mathbf{x}}_i - \bar{\mathbf{x}}_i\|^2, \quad (4)$$

where I is the set of all predefined target states. Furthermore, we support the generation of manageable and smooth trajectories by penalizing both high magnitudes and high changes in the control inputs throughout the entire time horizon. The corresponding cost can be written as

$$\ell_{\text{regularizer}}(\mathbf{u}) = \sum_{i=0}^{n-1} \|\mathbf{u}_i\|^2 + \sum_{i=1}^{n-1} \|\mathbf{u}_i - \mathbf{u}_{i-1}\|^2. \quad (5)$$

We incorporate bounds on the control inputs $\mathbf{u}_l \leq \mathbf{u}_i \leq \mathbf{u}_b \forall i$ based on the physical limits of the RC car in form of soft constraints

$$\ell_{limits}(\mathbf{u}) = \sum_{i=0}^{n-1} (B(-\mathbf{u}_i + \mathbf{u}_l) + B(\mathbf{u}_i - \mathbf{u}_b)), \quad (6)$$

where \mathbf{u}_l and \mathbf{u}_b denote the lower and upper bounds, respectively, and B is a one-sided quadratic barrier function.

C. Trajectory Optimization

We solve the trajectory optimization problem as stated in Eq. (3) by using a gradient descent batch approach. Hereby, we are interested in finding the optimal control parameters that minimize the total cost $\ell(\hat{\mathbf{x}}, \mathbf{u}) := \ell(\hat{\mathbf{x}}(\mathbf{u}), \mathbf{u})$, where $\hat{\mathbf{x}} := \hat{\mathbf{x}}(\mathbf{u})$ reflects the dynamics modeled by the state transition function f_θ for the entire trajectory. By following the chain rule, we can compute the gradient as

$$\frac{d\ell}{d\mathbf{u}} = \frac{\partial \ell}{\partial \hat{\mathbf{x}}} \frac{d\hat{\mathbf{x}}}{d\mathbf{u}} + \frac{\partial \ell}{\partial \mathbf{u}}. \quad (7)$$

To calculate the Jacobian $\frac{d\hat{\mathbf{x}}}{d\mathbf{u}}$, we follow the same procedure as described in [43]. First, we define the dynamics residual for one trajectory step i as

$$\mathbf{g}_i := \hat{\mathbf{x}}_{i+1} - f(\hat{\mathbf{x}}_i, \mathbf{u}_i) = 0, \quad (8)$$

and stack them into one vector for the entire trajectory $\mathbf{g} := (\mathbf{g}_0, \dots, \mathbf{g}_{n-1})$. Then, following the implicit function theorem, the Jacobian can be computed analytically by

$$\frac{d\hat{\mathbf{x}}}{d\mathbf{u}} = -\frac{\partial \mathbf{g}}{\partial \hat{\mathbf{x}}}^{-1} \frac{\partial \mathbf{g}}{\partial \mathbf{u}}. \quad (9)$$

We note that this can be computed efficiently by leveraging the block structure of the individual matrices (as discussed in [43]). Furthermore, since we are learning the state transition function in terms of local velocities (see Eq. (2)), we first compute the derivatives of $\hat{\mathbf{v}}$, and then transform them back into the global frame to receive the derivatives of $\hat{\mathbf{x}}$.

We pair this batch gradient descent formulation with a line search procedure, where we scale the gradient $\frac{d\ell}{d\mathbf{u}}$ with 512 different constants in the range of $[10^{-6}, 10^0]$. We simultaneously evaluate the resulting 512 new control vector candidates and pick the best solution based on the lowest total cost $\ell(\hat{\mathbf{x}}, \mathbf{u})$. We repeat this simple procedure for each iteration of the optimization until convergence.

An overview of the entire pipeline, including data collection, training, and trajectory optimization is given in Fig. 2.

IV. MODEL SELECTION

In this section, we describe the model selection process. We used our simulated car model to evaluate different neural network architectures on synthetic data. While network training solely relies on a loss over one time step, our goal is to learn a model that can match the dynamics of the car over an entire trajectory. To evaluate this performance, we use 40 pre-recorded validation trajectories with known end state poses. We infer the corresponding control trajectories on each learned model

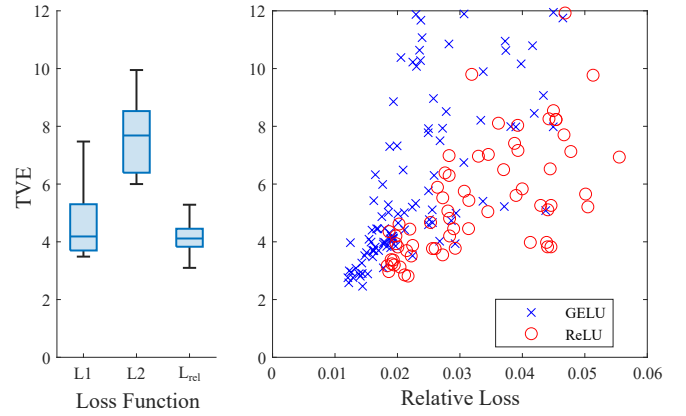


Fig. 3: Left: Comparison of distribution for TVE of different model architectures trained with respect to L1, L2 and L_{rel} (Eq. (11)) training losses. Right: Comparison of different model architectures with Rectified Linear Units (ReLU) or Gaussian Error Linear Units (GELU) activations on the L_{rel} loss and TVE (Eq. (10)).

candidate and compare the resulting end-state poses by computing the final state error. We denote the mean of all 40 final pose errors as *Trajectory Validation Error* (in short TVE), i.e.

$$\text{TVE} = \frac{1}{40} \sum_{j=0}^{40} \|\hat{\mathbf{x}}_n - \mathbf{x}_n^j\|_1, \quad (10)$$

where \mathbf{x}_n^j denotes the final state of a particular validation trajectory j . We use this as a metric to evaluate the efficacy of the different neural network architectures. We note that other evaluation metrics could also be applied, but we find that this one works well for our use case, as it essentially captures the accumulated state error throughout the trajectory.

A. Loss Function

During neural network training, choosing a suitable loss function is of utmost importance. Since we train on the relative velocities of the car, we encounter a high dynamic range. We expect that the most suitable models for trajectory inference are those that minimize the relative error of the training data. Our intuition is that the loss function should be more sensitive to absolute errors for small velocities. We tackle this by introducing the following relative loss for our training:

$$L_{rel}(\theta) = \frac{\|\mathbf{v}_{i+1} - f_\theta(\mathbf{v}_i, \mathbf{u}_i)\|_1}{\|\mathbf{v}_{i+1}\|_1 + \epsilon}, \quad (11)$$

where $\epsilon > 0$ prevents numerical problems for small velocities. We trained 15 multiple feed-forward and fully connected neural networks with 8 hidden layers and 64 neurons per layer with three loss functions: L1 loss, L2 loss and our relative loss. For each network, we inferred the validation trajectories and calculated the mean end distance (see Fig. 3 on the left). We found that networks trained with either L1 loss or relative loss perform notably better than those trained with L2 loss. Due to the lower variance, we use our relative loss for all further training.

B. Activation Functions and Network Size

Activation functions are used to capture nonlinearities with neural networks. Typical choices for activation functions are sigmoid, tanh, and ReLU. Nevertheless, sigmoid and tanh often suffer from the well-known exploding/vanishing gradients problem when trained with backpropagation [44]. To this end, ReLU is mostly preferred in the machine learning community. However, the gradient of ReLU is not continuous, which potentially imposes a challenge for gradient-based trajectory optimization. Particularly a neural network with ReLU activations may result in very noisy (i.e. fluctuating) control sequences when employed with trajectory optimization. As we want to apply the optimized control inputs directly to our physical system, this can have a negative impact on the overall performance, and could potentially even damage the hardware. Therefore, in this work, we also consider GELU [45] as a differentiable alternative to ReLU. We hypothesize that because GELU has continuous gradients, it could result in smoother control trajectories, which would make it better suited for our application. We further discuss this matter in section VI.

For selecting the network architecture (activation functions and size), we trained a total of over 200 neural networks of different sizes with both ReLU and GELU as activation functions (see Fig. 3 on the right). Furthermore, we performed a grid search with different network sizes for both activation functions (Fig. 4). Finally, we selected an architecture with 8 hidden layers of 64 neurons each with the GELU activation function based on two criteria (i) network size/evaluation time, and (ii) performance on TVE and test loss.

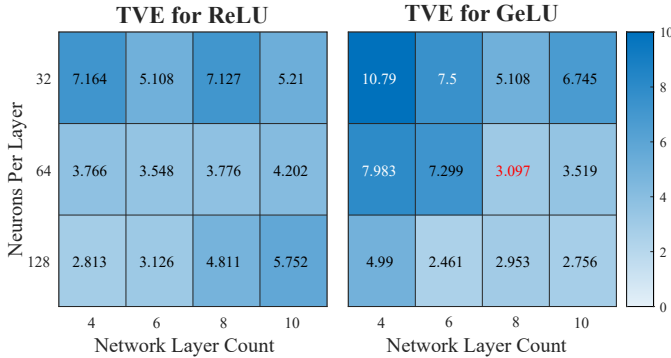


Fig. 4: Results from grid search for different network architectures with ReLU or GELU activations based on TVE (Eq. (10)).

V. RESULTS

We use the selected model architecture in combination with data recorded on the physical system to train a neural network that captures the dynamics of the real car. We evaluate the efficacy of our presented pipeline on a number of experiments, where we focus on generating *dynamic* driving behaviors through trajectory optimization. We present these experiments in the accompanying video and discuss them in the following.

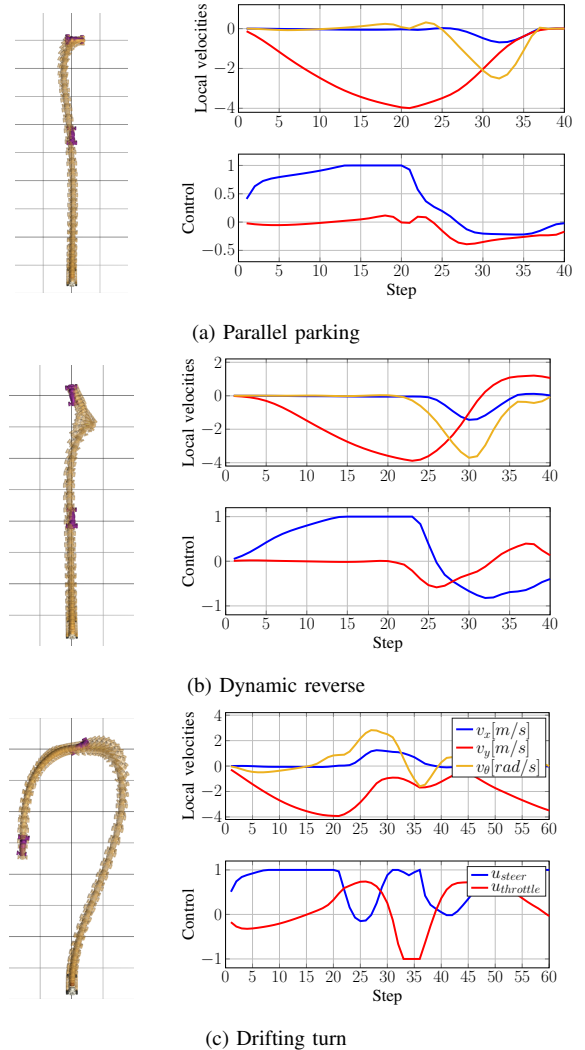


Fig. 5: Nominal trajectories (in orange) are based on optimization with our learned model for the three scenarios. The target states are marked in violet.

A. Offline Trajectory Optimization

We perform offline trajectory optimization for three different scenarios. We optimize, based on our learned model, a nominal trajectory and play it back on the physical system in an open-loop manner. All three scenarios included dynamic drifting maneuvers, and we refer to the individual experiments as: *Parallel Parking* (see Fig. 6), *Dynamic Reverse* (see Fig. 5b), and *Drifting Turn* (see Fig. 7). The scenarios were created by setting both an intermediate as well as an end-state goal using Eq. (4). For each scenario, we repeat the same experiment 20 times for slightly different starting positions. We execute the resulting optimal control trajectory on the physical car while recording its pose in the same manner as for data collection (see Fig. 8). We notice that while the executed trajectory matches the nominal trajectory in general, we accumulate errors over the length of the trajectory. Those errors can arise due to both aleatoric and epistemic uncertainties [46]. We encounter systematic errors in acceleration that lead, over the time horizon, to an offset in the mean end position (see table I).



Fig. 6: *Parallel Parking* experiment: The presented trajectory optimization method leverages the learned dynamics model of the physical car to dynamically park between two soda cans. The figure shows a sequence of several consecutive frames (left to right).

Table I: Error between the desired end-position and achieved end-position for open-loop trajectory optimization on different trajectories.

	Parallel Parking	Dynamic Reverse	Drifting Turn
Trajectory Length	40	40	60
Mean L2 Position Error [m]	0.38	0.21	0.37
STDev L2 Position Error [m]	0.10	0.074	0.21
Mean Absolute Heading Error [rad]	0.13	0.50	0.10
STDev Absolute Heading Error [rad]	0.08	0.10	0.10



Fig. 7: *Drifting Turn* experiment: The physical RC car takes a dynamic turn around a soda can by performing a controlled drifting maneuver (sequence top to bottom).

B. Online Trajectory Optimization

We also performed experiments in an online trajectory optimization setting by driving on a predefined race track (see Fig. 9). Hereby, we applied trajectory optimization in a receding horizon fashion, i.e. we reoptimized the control sequence at each control cycle, and applied the first control input to the physical system. We apply this feedback control scheme by leveraging the same motion capture system for data recording, where we include the measured state of the physical car as initial condition into the optimization. The overall objective (introduced as costs $\ell(x, u)$) is to advance along the race track with a predefined high velocity for the entire time horizon of the trajectory. Additionally, we add a cost for track excursions. Hereby, we choose a total of $n = 20$ trajectory steps and a framerate of 20 Hz. We note that our current implementation for the analytic computation of derivatives from the network is not optimized for run

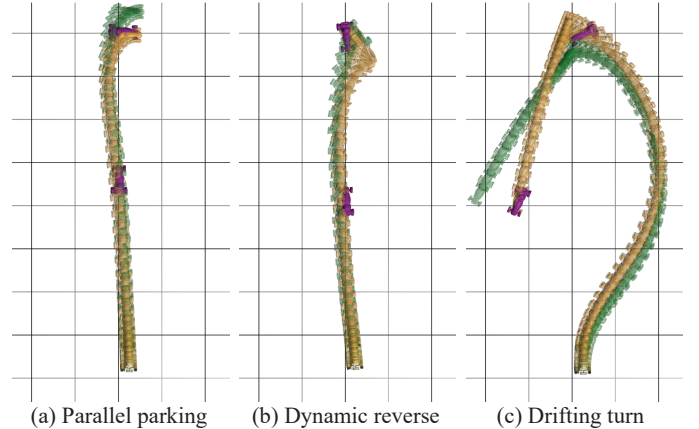


Fig. 8: Recorded examples (in green) of executed nominal trajectories (in orange) for the three scenarios. Target states are marked in violet. We encounter similar dynamic behavior on the RC car as our nominal trajectories, including drifts. Due to the open-loop control scheme, we accumulate an error over the length of the trajectories.

time, and we could therefore not run the optimization at a sufficiently high framerate. Instead, we leverage parallelization to compute finite differences that estimate the derivatives $\frac{d\phi}{du}$ for this particular experiment. Additional performance metrics of the RC car on the racetrack are given in Fig. 9. As shown in the video, the car is able to race through the track with high velocity while performing dynamic maneuvers. This demonstrates that error accumulations encountered in an offline setting can be successfully compensated by feedback control.

VI. DISCUSSION AND FUTURE WORK

Based on our experiments, we conclude that even simple network architectures can be used to reliably model the dynamics of a fast-driving RC car. Furthermore, the network and its derivatives can be successfully leveraged for gradient-based trajectory optimization. We showed that our pipeline generates feasible optimal control trajectories that can be directly applied to the physical car. Even though model inaccuracies can accumulate over the trajectory horizon, we note that the predicted behavior can nonetheless be reliably mimicked by the physical car. Furthermore, we addressed these problems using feedback control to complete a race track using dynamic maneuvers.

During our investigations to find a suitable activation function (see section IV-B), we hypothesized that the discontinuity of ReLU's gradients could lead to noisy control sequences when applied for trajectory optimization. This was the main

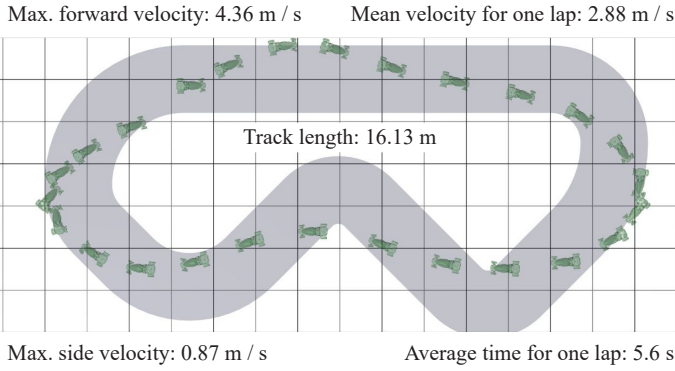


Fig. 9: The physical RC car (right) follows the control commands generated in a receding horizon fashion to dynamically drive on the race track. A recording of one entire lap is shown in the image on the left.

reason why we explored GELU as a possible alternative. Indeed, we validated this hypothesis throughout our experiments. As depicted in Fig. 10, the control sequence resulting from the network with GELU activations is considerably smoother than the one obtained using ReLU activations. We trace this back to the gradient used for trajectory optimization, which is much noisier for ReLU as well. Nonetheless, based on these observations we are currently unable to deduce which network architecture captures gradients of the real dynamics more accurately. Even though our proposed network results in smooth input sequences and achieves desirable performance for trajectory optimization, it might still fail to precisely represent gradients of the real system. Because the real gradients are not available during training on the real hardware, this is difficult to deduce. We speculate that receiving accurate (rather than just smooth) gradients might improve the convergence behavior of the trajectory optimization technique. A full-on investigation on this topic, including the analysis of structured learning techniques for capturing robot dynamics [47], is an exciting avenue for future work.

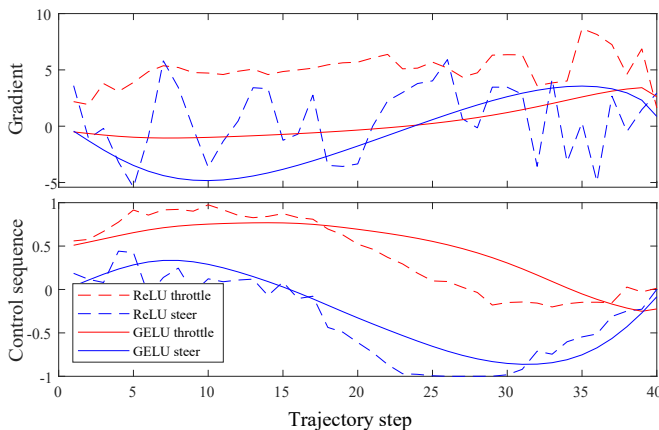


Fig. 10: Comparison of gradients $\frac{d\ell}{du}$ and control sequences u for neural network architectures with ReLU and GELU activations. The network with ReLU activations results in noisier (i.e. more fluctuating) gradients and input sequences than the network with ReLU activations.

We further note that traditional MBRL methods update the model with new rollouts collected after a policy evaluation step. In this work, we focused on learning the dynamics with minimal effort on data collection and training. Another possible extension to our work is to leverage continual learning to explore how additional data from the policy evaluation can improve our model’s performance.

We note that trajectory optimization techniques are known to exploit the inaccuracies of a model [25], [34]. This behavior was observed in our offline trajectory optimization experiments (section V-A). Approaches such as [25], [27] leverage the epistemic uncertainty of a family of models [46] to hinder such exploitations. We consider integrating such approaches into our framework in the future.

Finally, we are excited to investigate how our approach generalizes to other robotic systems, particularly for cases where no analytic model is available (such as for example [23]).

REFERENCES

- [1] F. Rubio, F. Valero, and C. Llopis-Albert, “A review of mobile robots: Concepts, methods, theoretical framework, and applications,” *International Journal of Advanced Robotic Systems*, vol. 16, no. 2, 2019.
- [2] S. Thrun, M. Montemerlo, H. Dahlkamp, D. Stavens, A. Aron, J. Diebel, P. Fong, J. Gale, M. Halpenny, G. Hoffmann, K. Lau, C. Oakley, M. Palatucci, V. Pratt, P. Stang, S. Strohband, C. Dupont, L.-E. Jendrossek, C. Koelen, C. Markey, C. Rummel, J. van Niekerk, E. Jensen, P. Alessandrini, G. Bradski, B. Davies, S. Ettinger, A. Kaehler, A. Nefian, and P. Mahoney, *Stanley: The Robot That Won the DARPA Grand Challenge*. Berlin, Heidelberg: Springer Berlin Heidelberg, 2007, pp. 1–43.
- [3] M. Blösch, S. Weiss, D. Scaramuzza, and R. Siegwart, “Vision based map navigation in unknown and unstructured environments,” in *2010 IEEE International Conference on Robotics and Automation*, 2010, pp. 21–28.
- [4] C. Gehring, S. Coros, M. Hutter, C. Dario Bellicoso, H. Heijnen, R. Dietelm, M. Bloesch, P. Fankhauser, J. Hwangbo, M. Hoepfinger, and R. Siegwart, “Practice makes perfect: An optimization-based approach to controlling agile motions for a quadruped robot,” *IEEE Robotics Automation Magazine*, vol. 23, no. 1, pp. 34–43, 2016.
- [5] J. Lee, J. Hwangbo, L. Wellhausen, V. Koltun, and M. Hutter, “Learning quadrupedal locomotion over challenging terrain,” *Science Robotics*, vol. 5, no. 47, p. eabc5986, 2020.
- [6] L. Biagiotti and C. Melchiorri, *Trajectory Planning for Automatic Machines and Robots*, 1st ed. Springer Publishing Company, Incorporated, 2008.
- [7] M. Geilinger, R. Poranne, R. Desai, B. Thomaszewski, and S. Coros, “Skaterbots: Optimization-based design and motion synthesis for robotic creatures with legs and wheels,” in *Proceedings of ACM SIGGRAPH, A. T. on Graphics (TOG), Ed.*, vol. 37. ACM, August 2018.

- [8] J. M. Bern, P. Banzet, R. Poranne, and S. Coros, "Trajectory optimization for cable-driven soft robot locomotion," *Robotics: Science and Systems XV*, 2019.
- [9] S. Zimmermann, R. Poranne, J. M. Bern, and S. Coros, "PuppetMaster," *ACM Transactions on Graphics*, vol. 38, no. 4, pp. 1–11, 2019.
- [10] D. Harsh and B. Shyrokau, "Tire model with temperature effects for formula sae vehicle," *Applied Sciences*, vol. 9, no. 24, 2019.
- [11] K. Åström and P. Eykhoff, "System identification - a survey," *Automatica*, vol. 7, no. 2, pp. 123–162, 1971.
- [12] L. Ljung, *System Identification*. John Wiley & Sons, Ltd, 1999.
- [13] D. Nguyen-Tuong and J. Peters, "Model learning for robot control: a survey," *Cognitive Processing*, vol. 12, no. 4, pp. 319–340, 2011.
- [14] K. Hornik, M. Stinchcombe, and H. White, "Multilayer feedforward networks are universal approximators," *Neural Networks*, vol. 2, no. 5, pp. 359–366, 1989.
- [15] J. Z. Kolter, C. Plagemann, D. T. Jackson, A. Y. Ng, and S. Thrun, "A probabilistic approach to mixed open-loop and closed-loop control, with application to extreme autonomous driving," in *2010 IEEE International Conference on Robotics and Automation*, 2010, pp. 839–845.
- [16] A. Liniger, A. Domahidi, and M. Morari, "Optimization-based autonomous racing of 1:43 scale rc cars," *Optimal Control Applications and Methods*, vol. 36, no. 5, p. 628–647, Jul 2014.
- [17] T. M. Moerland, J. Broekens, and C. M. Jonker, "Model-based reinforcement learning: A survey," 2021.
- [18] L. P. Kaelbling, M. L. Littman, and A. W. Moore, "Reinforcement learning: A survey," *J. Artif. Int. Res.*, vol. 4, no. 1, p. 237–285, may 1996.
- [19] M. P. Deisenroth and C. E. Rasmussen, "Pilco: A model-based and data-efficient approach to policy search," in *Proceedings of the 28th International Conference on Machine Learning*, ser. ICML'11. Madison, WI, USA: Omnipress, 2011, p. 465–472.
- [20] M. P. Deisenroth, D. Fox, and C. E. Rasmussen, "Gaussian processes for data-efficient learning in robotics and control," *IEEE Transactions on Pattern Analysis and Machine Intelligence*, vol. 37, no. 2, pp. 408–423, 2015, journal impact factor 9.455. Highest Impact Journal in Machine Learning.
- [21] S. Kamthe and M. P. Deisenroth, "Data-efficient reinforcement learning with probabilistic model predictive control," in *Proceedings of the International Conference on Artificial Intelligence and Statistics (AISTATS)*, 2018.
- [22] J. Kabzan, L. Hewing, A. Liniger, and M. N. Zeilinger, "Learning-based model predictive control for autonomous racing," *IEEE Robotics and Automation Letters*, vol. 4, pp. 3363–3370, 2019.
- [23] S. Zimmermann, R. Poranne, and S. Coros, "Go fetch! - dynamic grasps using boston dynamics spot with external robotic arm," in *2021 IEEE International Conference on Robotics and Automation (ICRA)*, 2021, pp. 4488–4494.
- [24] A. Nagabandi, G. Kahn, R. S. Fearing, and S. Levine, "Neural network dynamics for model-based deep reinforcement learning with model-free fine-tuning," in *2018 IEEE International Conference on Robotics and Automation (ICRA)*, 2018, pp. 7559–7566.
- [25] K. Chua, R. Calandra, R. McAllister, and S. Levine, "Deep reinforcement learning in a handful of trials using probabilistic dynamics models," in *Advances in Neural Information Processing Systems*, S. Bengio, H. Wallach, H. Larochelle, K. Grauman, N. Cesa-Bianchi, and R. Garnett, Eds., vol. 31. Curran Associates, Inc., 2018.
- [26] A. Nagabandi, K. Konolige, S. Levine, and V. Kumar, "Deep dynamics models for learning dexterous manipulation," in *Proceedings of the Conference on Robot Learning*, ser. Proceedings of Machine Learning Research, L. P. Kaelbling, D. Kragic, and K. Sugiura, Eds., vol. 100. PMLR, 30 Oct–01 Nov 2020, pp. 1101–1112.
- [27] S. Curi, F. Berkenkamp, and A. Krause, "Efficient model-based reinforcement learning through optimistic policy search and planning," in *Advances in Neural Information Processing Systems*, H. Larochelle, M. Ranzato, R. Hadsell, M. F. Balcan, and H. Lin, Eds., vol. 33. Curran Associates, Inc., 2020, pp. 14 156–14 170.
- [28] C. E. Rasmussen and C. K. I. Williams, *Gaussian Processes for Machine Learning (Adaptive Computation and Machine Learning)*. The MIT Press, 2005.
- [29] R. Calandra, J. Peters, C. E. Rasmussen, and M. P. Deisenroth, "Manifold gaussian processes for regression," in *Proceedings of the IEEE International Joint Conference on Neural Networks (IJCNN)*, 2016.
- [30] J. Fu, S. Levine, and P. Abbeel, "One-shot learning of manipulation skills with online dynamics adaptation and neural network priors," in *2016 IEEE/RSJ International Conference on Intelligent Robots and Systems (IROS)*. IEEE Press, 2016, p. 4019–4026.
- [31] M. Henaff, W. F. Whitney, and Y. LeCun, "Model-based planning with discrete and continuous actions," *arXiv preprint arXiv:1705.07177*, 2017.
- [32] N. Mishra, P. Abbeel, and I. Mordatch, "Prediction and control with temporal segment models," in *Proceedings of the 34th International Conference on Machine Learning*, ser. Proceedings of Machine Learning Research, D. Precup and Y. W. Teh, Eds., vol. 70. PMLR, 06–11 Aug 2017, pp. 2459–2468.
- [33] J. M. Bern, Y. Schneider, P. Banzet, N. Kumar, and S. Coros, "Soft Robot Control With a Learned Differentiable Model," in *2020 3rd IEEE International Conference on Soft Robotics (RoboSoft)*, 2020, pp. 417–423.
- [34] A. Byravan, J. T. Springenberg, A. Abdolmaleki, R. Hafner, M. Neunert, T. Lampe, N. Siegel, N. Heess, and M. Riedmiller, "Imagined value gradients: Model-based policy optimization with transferable latent dynamics models," in *Proceedings of the Conference on Robot Learning*, ser. Proceedings of Machine Learning Research, L. P. Kaelbling, D. Kragic, and K. Sugiura, Eds., vol. 100. PMLR, 30 Oct–01 Nov 2020, pp. 566–589.
- [35] D. Hafner, T. Lillicrap, J. Ba, and M. Norouzi, "Dream to control: Learning behaviors by latent imagination," 2020.
- [36] Z. I. Botev, D. P. Kroese, R. Y. Rubinstein, and P. L'Ecuyer, "Chapter 3 - the cross-entropy method for optimization," in *Handbook of Statistics*, ser. Handbook of Statistics. Elsevier, 2013, vol. 31, pp. 35–59.
- [37] H. Bharadhwaj, K. Xie, and F. Shkurti, "Model-predictive control via cross-entropy and gradient-based optimization," in *Proceedings of the 2nd Conference on Learning for Dynamics and Control*, ser. Proceedings of Machine Learning Research, A. M. Bayen, A. Jadbabaie, G. Pappas, P. A. Parrilo, B. Recht, C. Tomlin, and M. Zeilinger, Eds., vol. 120. PMLR, 10–11 Jun 2020, pp. 277–286.
- [38] C. E. Garc a, D. M. Prett, and M. Morari, "Model predictive control: Theory and practice - a survey," *Automatica*, vol. 25, no. 3, pp. 335–348, 1989.
- [39] S. Levine and P. Abbeel, "Learning neural network policies with guided policy search under unknown dynamics," in *Advances in Neural Information Processing Systems*, Z. Ghahramani, M. Welling, C. Cortes, N. Lawrence, and K. Q. Weinberger, Eds., vol. 27. Curran Associates, Inc., 2014.
- [40] W. Li and E. Todorov, "Iterative linear quadratic regulator design for nonlinear biological movement systems," in *ICINCO (1)*. INSTICC Press, 2004, pp. 222–229.
- [41] R. Peppy, A. Lambert, and H. Mounier, "Path planning using a dynamic vehicle model," in *2006 2nd International Conference on Information Communication Technologies*, vol. 1, 2006, pp. 781–786.
- [42] W. H. Press and S. A. Teukolsky, "Savitzky-Golay Smoothing Filters," *Computers in Physics*, vol. 4, no. 6, pp. 669–672, 1990.
- [43] S. Zimmermann, R. Poranne, and S. Coros, "Optimal control via second order sensitivity analysis," *arXiv:1905.08534 [math]*, May 2019, arXiv: 1905.08534.
- [44] S. Hochreiter, "Untersuchungen zu dynamischen neuronalen Netzen. Diploma thesis, Institut für Informatik, Lehrstuhl Prof. Brauer, Technische Universität München," Ph.D. dissertation, Technische Universität München, 1991.
- [45] D. Hendrycks and K. Gimpel, "Gaussian error linear units (gelus)," *arXiv preprint arXiv:1606.08415*, 2016.
- [46] E. Hüllermeier and W. Waegeman, "Aleatoric and epistemic uncertainty in machine learning: an introduction to concepts and methods," *Machine Learning*, vol. 110, no. 3, pp. 457–506, 2021.
- [47] A. R. Geist and S. Trimpe, "Structured learning of rigid-body dynamics: A survey and unified view from a robotics perspective," *GAMM-Mitteilungen*, vol. 44, no. 2, p. e202100009, 2021.